ELSEVIER

International Journal of Pharmaceutics 227 (2001) 39–46

international journal of pharmaceutics

www.elsevier.com/locate/ijpharm

The determination of fracture mechanics properties of pharmaceutical materials in mode III loading using an anti-clastic plate bending method

Fridrun Podczeck *

Department of Pharmaceutics, The School of Pharmacy, University of London, 29/39 Brunswick Square, London WC1N 1AX, UK

Received 6 January 2001; received in revised form 5 February 2001; accepted 11 February 2001

Abstract

Powder compacts made from acetylsalicylic acid and lactose monohydrate were subjected to an anti-clastic plate bending method in order to obtain the critical stress intensity factor in mode III loading (tearing or antiplane shear mode). The theoretical approach for data processing was based on linear elastic fracture mechanics. In contrast to mode I loading (opening or tensile mode), where above a critical threshold value the critical stress intensity factor is independent of the notch depth, i.e. converts into a true material constant, in mode III loading the critical stress intensity factor could only be presented under strict reference to a defined notch length. For lactose monohydrate, the typical exponential relationship between critical stress intensity factor and plate porosity was found. However, this was not the case for acetylsalicylic acid plates, indicating a change in fracture origin from pores and clusters of pores at higher porosities to machine flaws at low porosities. Hence, no extrapolation to zero porosity was attempted for this material, whereas for lactose monohydrate, the critical stress intensity factor at zero porosity was estimated to be 102 ± 14 MNm$^{3/2}$. This value is valid for a notch depth of 4.9 ± 0.3 mm. From the values obtained for the critical stress intensity factor and the critical strain energy release rate in mode III loading and an anisotropy ratio, here defined as the ratio between the critical stress intensity factors obtained in mode I and mode III loading, it was concluded that acetylsalicylic acid is the more brittle material and that lactose monohydrate behaved rather ductile under the given experimental conditions.

Keywords: Acetylsalicylic acid; Anti-clastic plate bending; Critical stress intensity factor; Fracture mechanics; Mode III loading; Lactose monohydrate

1. Introduction

Crack propagation and the theory of fracture mechanics are the foundation of modern fracture science and are of utmost importance for pharmaceutical processes, such as tabletting, tablet strength testing and other issues involving adhe-

* Tel./fax: +44-20-7753-5857.

E-mail address: fridrun.podczeck@ams1.ulsop.ac.uk (F. Podczeck).

0378-5173/01/$ - see front matter
PII: S0378-5173(01)00783-9

sion and friction between individual powder particles. In order to arrive at a continuum stress analysis for plane-cracks in specimens, such as tablets, usually three basic modes of crack-surface displacement are distinguished. These are mode I—the opening or 'tensile' mode—corresponding to normal separation of the crack walls under the influence of tensile stress; mode II—the sliding or 'in-plane shear' mode—which reflects a longitudinal shearing of the crack walls in a direction normal to the crack front; and mode III—the tearing or 'antiplane shear' mode—in which a lateral shearing parallel to the crack front takes place. These three basic modes are illustrated in Fig. 1.

One important characteristic of powder compacts is their brittleness, i.e. fracture is not preceded by significant deformation (Stanley, 1985). A fracture mechanics approach to describe the mechanical failure of tablets is hence required. Such a concept was first introduced into the pharmaceutical literature by Mashadi and Newton (1987a,b, 1988). Cracks in brittle specimens are most likely to propagate under the influence of tensile stresses, for example during diametral tensile strength testing (Fell and Newton, 1968). It is hence not surprising that so far, attention has been paid only to mode I of crack-surface displacement, i.e. the tensile mode, as can be seen from recent reviews (Rowe and Roberts, 1995; Bin Baie et al., 1996). However, Fell and Newton (1970), when comparing spray-dried and crystalline lactose, also observed shear failure for the former material under certain test conditions. This indicates an influence of the materials from which tablets are made on the stresses developing in compacts when these are handled. It hence appears important to characterise materials used in pharmaceutical powder compacts in different modes of failure with the aim to develop a 'fracture envelope'. The fracture envelope represents the strength characteristics of a particular material under different stress situations and offers a rational basis for the comparison and evaluation of the mechanical properties of anisotropic powder compacts (Stanley, 1985). The knowledge of fracture mechanics parameters determined in different modes of failure also opens the possibility for a theoretical approach to the prediction of tablet strength (Johnson, 1997). The aim of this work was to determine fracture mechanics parameters in mode III for two model powders—acetylsalicylic acid (ASS) and lactose monohydrate (LM). For these two powders, the mode I fracture mechanics properties had been evaluated previously (Podczeck, 2001) in comparison to Young's modulus and tablet tensile strength. So far in the pharmaceutical literature, a mode III evaluation has not been attempted for any material or specimen geometry and also in the engineering literature, methods producing a pure mode III fracture are rarely reported.

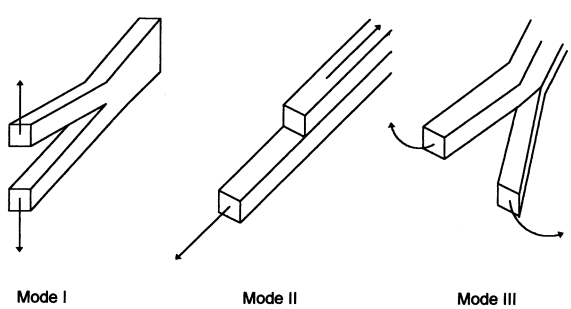

Fig. 1. Basic modes of crack-surface displacement: mode I, i.e. opening or tensile mode; mode II, i.e. sliding or in-plane shear mode; mode III, i.e. tearing or antiplane shear mode.

2. Anti-clastic plate bending (ACPB) method

Farshad and Flüeler (1998) reported a new test methodology for mode III fracture, which assures a relatively pure tearing stress field. The method is simple enough to be adapted to the needs of pharmaceutical powder specimens and there is a theoretical approach for data processing provided based on a valid model (linear elastic fracture mechanics). During ACPB, a rectangular plate undergoes a twisting type of deformation. The plate assumes a saddle-shape resulting in two opposite curvatures and tearing the plate apart. In Fig. 2, the general loading configuration and the plate and crack geometry are illustrated.

Both mode II and mode III failure occur due to shear and hence, the elastic plate theory can be

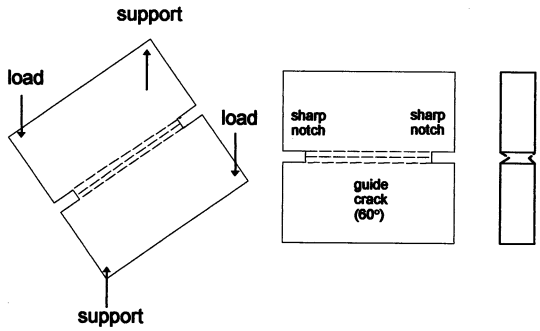

Fig. 2. Specimen and loading configuration for compacts used to determine fracture mechanics properties in mode III loading. Left: the corners of one diagonal of the specimen are loaded equally, whereas the two corners of the other diagonal are placed onto a rigid support. Middle/right: the sharp notches extend from the edge of the specimen towards the middle and pass fully through the specimen thickness. The guide cracks (60°) connect the sharp notches on both sides of the specimen without penetrating into the plane surfaces of the specimen by more than 500–600 μm.

employed to derive different fracture mechanics properties, finally leading to a critical stress intensity factor in mode III. During loading of the plates in the configuration shown in Fig. 2, the plates will deflect and this deflection is measured at the loaded corners. Determining the exact amount of deflection enables the calculation of the 'in-plane shear modulus' G^{II} from (Farshad et al., 1997):

$$G^{II} = \frac{3Fb^2}{2\delta h^3} \quad (1)$$

where F is the load applied at the corners of the plate, b is the length of the square-shaped plate, h, the thickness of the plate and δ, the measured displacement of the loaded corners. This shear value is required for the calculation of the critical stress intensity factor in mode III, as is the critical strain energy release rate in mode III, G_{IC}^{III}:

$$G_{IC}^{III} = \frac{F^2}{2h}\frac{\partial C}{\partial a} \quad (2)$$

where C is the elastic plate compliance and a, the length of the sharp notch (see Fig. 2).Roark (1965) has defined the elastic plate compliance C as follows:

$$C = \frac{\Delta}{F} \quad (3)$$

where Δ is the deflection of the corners, which can here be estimated from:

$$\Delta = b\theta \quad (4)$$

with

$$\theta = \frac{FBb}{2G^{II}J} \quad (5)$$

and

$$J = \frac{1}{16}Bh^3\left[\frac{16}{3} - 3.36\frac{h}{B}\left(1 - \frac{h^4}{12B^4}\right)\right] \quad (6)$$

where θ is the angle of twist, B is the ligament thickness, i.e. $B = b - 2a$ and J, the calibration value. The product $G^{II}J$ defines the torsional rigidity of the plates.

The change of the elastic plate compliance as a function of the notch depth ($\partial C/\partial a$ in Eq. (2)) must be determined experimentally. The critical stress intensity factor in mode III, K_{IC}^{III}, can then be calculated from:

$$K_{IC}^{III} = \sqrt{2G^{II}G_{IC}^{III}} \quad (7)$$

3. Materials and methods

The following powders were used: acetylsalicylic acid (ASS, Rütgers Organics GmbH, CF Aubing Pharmaceuticals, Mannheim, Germany, batch 98070230), lactose monohydrate (LM, Borculo Whey Products, Saltney, UK, batch 826704). The particle size was determined using light microscopy (Olympus BH-2, Tokyo, Japan) in connection with image analysis (Seescan Solitaire 512, Cambridge, UK). One thousand particles were inspected and the mean Feret diameter was determined to be 8.8 ± 4.8 and 6.1 ± 3.9 μm for ASS and LM, respectively. The particle density was determined with an air pycnometer (Model 930, Beckman Instruments Inc., USA) and is 1540 ± 1 and 1400 ± 2 kg m^{-3} for LM and ASS, respectively (arithmetic mean and S.D. of five replicates).

The compacted powder specimens were manufactured on an Instron TT universal testing ma-

chine (Instron, High Wycombe, UK) at a compaction rate of 1 mm min^{-1} and on a hydraulic press (Specac 15,000, Specac Ltd., Kent, UK). The specimens were compacted to have a thickness of 5 mm after removal from the die. The compaction forces were recorded using an X-Y recorder (Gould, model 6000, Bryan Southern Ltd., Surrey, UK). Different beam porosities were achieved by varying the specimen weight.

A specially manufactured split-die system was used, which can be dissembled completely, as long as the pressure exerted by the powder compact allows opening. The nominal dimensions of the die are 20×20 mm. With a target thickness of 5 mm to have specimens comparable to previous work (Podczeck, 2001), the nominal volume of the specimens is 2.0 cm^3. For the calibration experiments (determination of the notch depth) 30 compacts with a porosity of 0.2 were produced. For all other experiments, 32 (LM) or 38 (ASS) compacts were manufactured, whereby the porosity of the specimens after unloading was between 0.2 and 0.05 (ASS) and between 0.2 and 0.07 (LM).

For the determination of the critical stress intensity factor in mode III the guide cracks (see Fig. 2) were inserted with a miniature file with a 60° opening angle, whereas the sharp notches for crack propagation were introduced into the plates using a Japanese pull saw. The depth of the guide cracks was ≈ 500–600 μm, whereas the notch depth varied between 1 and 9 mm extending from the edge of the specimen towards the middle. The notch depth on either side of the plate was measured using an image analysis system (Seescan Sonata, Cambridge, UK) connected to a zoom-lens (Olympus, Tokyo, UK). For calculations, the average of the two notch depths was used. The average pixel error was determined to be ± 66.8 μm.

The critical corner load of the plates was obtained on a universal strength tester (CT-5, Engineering Systems, Nottingham, UK) at a test speed of 1 mm min^{-1} using a 5 kg load cell. A bending rig with a specially designed loading attachment was used. The corner beam deflection was obtained from a chart recorder (see above) attached to the CT-5. All force-displacement profiles were fully linear until sudden and catastrophic failure of the specimens occurred. Hence, under the test conditions described, the compacts behaved in a brittle manner in all cases.

All beams were stored for at least 2 weeks at room temperature and 40–45% relative humidity of air. Before the experiments (24 h), the specimens were transferred into a desiccator filled with saturated solution of magnesium nitrate (BDH, Poole, UK), i.e. stored under controlled humidity of 53%. Afterwards, the specimens were weighed (electronic recording balance; Sartorius, Göttingen, Germany) and measured (electronic callipers; length ± 0.01 mm; width and thickness ± 0.001 mm). The porosity of the specimens was calculated from these data and the density of the materials. The notches were inserted and measured as described above and the breaking load was determined. All calculations were undertaken using SPSS 10.0 (SPSS Inc, Woking, UK). Non-linear relationships were always treated with non-linear regression to minimise errors when obtaining extrapolations to zero porosity.

4. Results and discussion

The ACPB method used to determine the critical stress intensity factor in mode III loading is fairly new and so far simulations or experimental results to the influence of specimen dimensions and geometry and depth of the guide cracks have not been reported in the literature. In this work, the specimen thickness was kept constant at 5 mm because this value had been used in previous experiments to determine the Young's modulus and the critical stress intensity factor in mode I loading using powder beams.

The two materials have been chosen for their different mechanical and tabletting properties. ASS is usually described as ductile material with large degree of plastic deformation (Humbert-Droz et al., 1983; Jetzer et al., 1984). However, at higher tabletting forces predominant elastic deformation was also reported (Mielck and Stark, 1995). Large ASS crystals cannot be compacted into tablets, whereas fine powder particles provide mechanically appropriate tablets when compressed at a low tabletting velocity. A change in

the crystal density during compression at higher loads was suspected (Pedersen and Kristensen, 1994) but remained unproven. For LM, the findings are somewhat contradicting as both ductility (Duberg and Nyström, 1982) and brittleness (Cole et al., 1975; Mielck and Stark, 1995) during compression has been reported. LM crystals appear to be more than six times as hard as ASS crystals. The indentation hardness values reported are 87 MPa (Ridgway et al., 1969) and 523 MPa (Ichikawa et al., 1988) for ASS and LM, respectively.

In Eq. (2), the change of the elastic plate compliance as a function of the notch depth ($\partial C/\partial a$) is introduced to remove the gross influence of the specimen geometry and the notch depth on the final results. It can be assumed that an increase in notch depth a changes the value of C to a larger extent, if the specimen is comparatively porous and of a general weak structure. Hence, to obtain a suitable value for the term $\partial C/\partial a$, calibration plates of a nominal porosity of 0.20 were prepared and the notch depth was varied between 1 and 9 mm. However, specimens with the two equal notches, each being deeper than 8.5 mm, cracked during introduction of the second notch. In Fig. 3, the elastic plate compliance is drawn as a function of the notch depth of the plates. In the range from 1 to just over 5 mm (ASS) or 6.6 mm

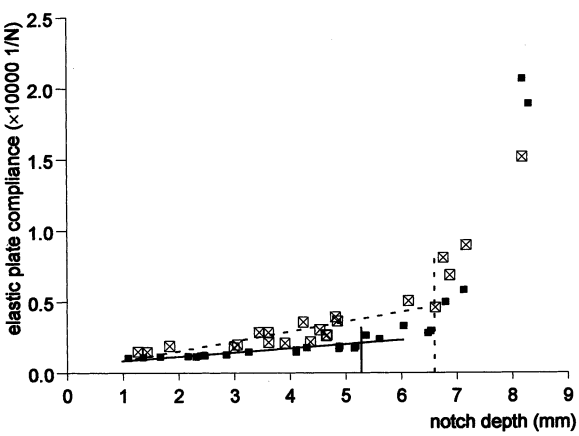

Fig. 3. Elastic plate compliance as a function of the notch depth for ASS (■) and LM (⊠). End of proportionality between elastic plate compliance and notch depth for ASS at ≈5.3 and 6.6 mm for LM.

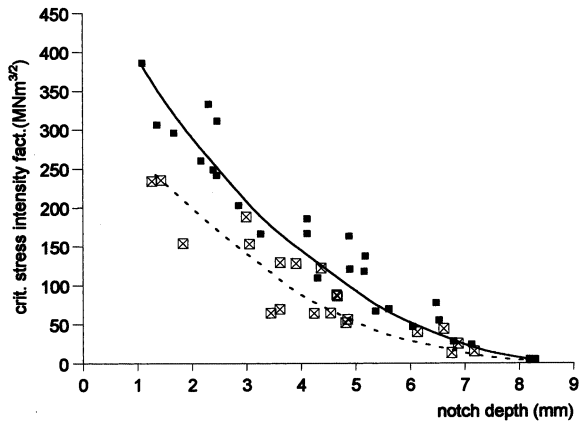

Fig. 4. Critical stress intensity factor in mode III loading as a function of notch depth for specimen of a nominal porosity of 0.2, ASS (■) and LM (⊠).

(LM), there is a proportionality between the two properties and hence a value for $\partial C/\partial a$ can be obtained from the slope in this range of notch depths. The values derived were 2.032×10^{-3} N^{-1} and 4.989×10^{-3} N^{-1} for ASS and LM, respectively. In this work it is assumed that the values for $\partial C/\partial a$ observed on powder plates of a nominal porosity of 0.2 are valid for plates of lower porosity, as this was the assumption made by Farshad and Flüeler (1998).

To determine the critical stress intensity factor in mode I it is important to determine the minimum notch depth in relation to the specimen geometry and in particular specimen thickness (Podczeck, 2001). Although this was not further studied by Farshad and Flüeler (1998), the notch depth will certainly have an influence on the crack propagation during the test. Whether there is, however, a minimum notch depth above which the values of the critical stress intensity factor become independent of notch depth, was investigated in Fig. 4 using the results from the calibration plates. Fig. 4 suggests that, although the elastic plate compliance should have removed the influence of notch depth on the critical stress intensity factor at least above a critical threshold value, there is a strong relationship between these two entities over the full range of notch depths tested. Farshad and Flüeler (1998) reported a

similar relationship, yet did not comment. It appears that the determination of the critical stress intensity factor in mode III is hence only possible under strict reference to a defined notch depth. Thus, to determine the critical stress intensity factor for plates of varying porosity, the notch depth was set close to the upper threshold values obtained from Fig. 3. For ASS, the experimental notch depth was then determined to be 4.7 ± 0.2 mm and for LM a notch depth of 4.9 ± 0.3 mm was employed.

In Fig. 5 the critical stress intensity factor in mode III loading is compared for the two materials as a function of plate porosity. For LM, the relationship follows an exponential function of the type $K_{IC} = K^0_{IC} \times e^{(-b \times \text{porosity})}$ closely, and the value for K^{III}_{IC} at zero porosity (K^0_{IC}) is 102 ± 14 $MNm^{3/2}$ (constant b 12.4 ± 1.0; $R^2 = 0.898$, residual analysis RMS = 6.3 $MNm^{3/2}$). Such exponential relationships between porosity and any mechanical property of porous powder specimens are typical (Rice, 1994). They are the result of a random pore structure and there is no change in relative flaw sizes or pore shapes with a decrease in specimen porosity.

A different picture emerges for ASS, for which the relationship between the values of the critical stress intensity factor and the plate porosity is not exponential (Fig. 5). A similar behaviour had been found for the Young's modulus but not for

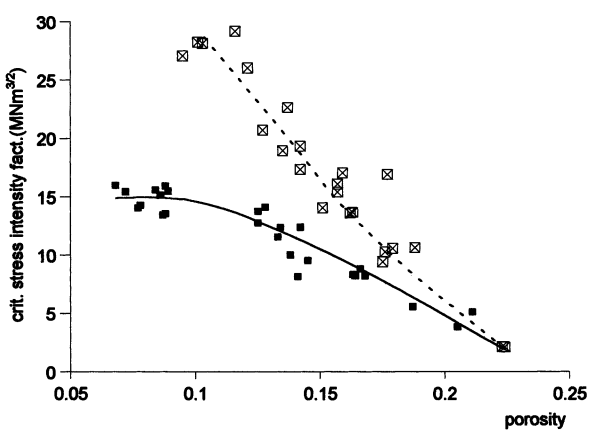

Fig. 5. Critical stress intensity factor in mode III loading as a function of the specimen porosity for ASS (■) and LM (⊠).

the critical stress intensity factor in mode I loading (Podczeck, 2001). This clearly demonstrates the anisotropy of powder specimens produced by uniaxial compression. It also suggests that the inner structure responsible for the elasticity of the plates is also stressed when determining the critical stress intensity factor in mode III loading, whereas in mode I loading, another set of flaws and pores is tested. The deviation from an exponential relationship could be an indication for a change in the origin of crack propagation at porosities below a value of ≈ 0.1. At lower porosities, the specimens showed increased relaxation and the compaction pressure required to produce a thickness of 5 mm and the target porosity after removal of the specimens from the die increased rapidly. The greater extent of elastic recovery could have resulted in internal rupture and as a consequence, larger flaws than pores and clusters of pores would normally provide. The change from pores and clusters of pores to such flaws as the origin of crack propagation could be the reason for the unusual relationship found. That such an unusual relationship had not been observed in mode I loading (Podczeck, 2001) could be the result of a preferred orientation of these flaws, presumably parallel to the plane surfaces of the specimens. It can be assumed that a further decrease in porosity would result in a second exponential part, as was observed for the changes in the Young's modulus as a function of specimen porosity (Podczeck, 2001). However, a further decrease in plate porosity was impossible under the restricted experimental opportunities available and hence, the likely second exponential portion of the critical stress intensity factor-porosity function could not be obtained. Hence, an extrapolation to zero-porosity as achieved for LM was not attempted. All that can be said is that the critical stress intensity factor in mode III loading for ASS is larger than 15.1 ± 0.8 $MNm^{3/2}$ (mean and S.D. of all values obtained from plates with a porosity below 0.1). From the graph (Fig. 5) it can be seen that, in general, the critical stress intensity factor of ASS is lower than that of LM and hence ASS is more brittle than LM when tested in mode III loading.

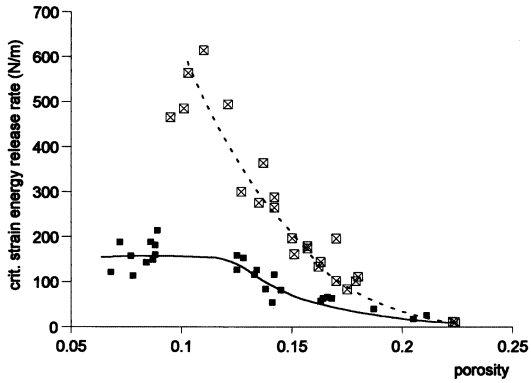

Fig. 6. Critical strain energy release rate in mode III loading as a function of the specimen porosity for ASS (■) and LM (⊠).

An anisotropy ratio can be defined from the ratio between the critical stress intensity factors obtained in mode I and mode III loading. For ASS, the reference value for a porosity of 0.7 is 210 $kNm^{3/2}$ in mode I loading and for LM the critical stress intensity factor in mode I loading at zero porosity is 493 $kNm^{3/2}$ (Podczeck, 2001). The anisotropy ratios are thus 0.0139 and 0.0048 for ASS and LM, respectively. Anisotropy is typical for compacts made by uniaxial compression, but the degree of anisotropy depends on stress transmission through the powder column in axial and radial direction. A larger degree of anisotropy indicates an imbalance in stress transmission and can, in the extreme, lead to lamination of the compact after ejection from the die. The results indicate that such problems might be more likely for LM than for ASS.

In Fig. 6, the critical strain energy release rates in mode III loading are drawn as a function of the plate porosity. Again, LM follows the typical exponential relationship ($G_{IC}^{III} = 3.6 \pm 0.8$ kN m^{-1}; $R^2 = 0.862$; RMS = 0.7 kN m^{-1}). ASS, however, shows a plateau value (0.16 ± 0.03 kN m^{-1}) at low values of plate porosity. This was expected as G_{IC} and K_{IC} are related physical properties (Griffith, 1920; Menčík, 1992). The results are larger than those reported for mode I loading (Podczeck, 2001). Hence, more elastic energy developed during crack propagation if the specimens were twisted rather than subjected to a plane tensile stress.

5. Conclusions

In contrast to mode I loading, where, above a critical threshold value, the critical stress intensity factor is independent of the notch depth, i.e. converts into a true material constant, in mode III loading the critical stress intensity factor can only be presented under strict reference to a defined notch depth. This will be important in particular for multiple layer tablets, as, when these are subjected to strength testing, a mixed mode failure will occur.

ASS plates change their inner structure with an increase in compaction pressure, presumably due to an increase in elastic recovery and related inner rupture and crack formation. As a result, the fracture origin during mode III loading appears to change from pores and clusters of pores at higher porosities to the flaws formed due to increased elastic recovery at porosities below 0.1. In such cases, an extrapolation to a zero porosity value appears inappropriate.

From the values obtained for the critical stress intensity factor and the critical strain energy release rate in mode III and the anisotropy ratio (ratio of critical stress intensity factor in mode I to that of mode III) it can be concluded that ASS is the comparatively more brittle material, but that LM is more likely to show lamination at smaller compact porosities.

Acknowledgements

This work was partly financed by the Deutsche Forschungsgemeinschaft via a Heisenberg-Fellowship. ASS and LM were gifts from Rütgers Organics GmbH, CT Aubing Pharmaceuticals (Mannheim, Germany) and Borculo Whey Products (Saltney, UK), respectively.

References

Bin Baie, S., Newton, J.M., Podczeck, F., 1996. The characterisation of the mechanical properties of pharmaceutical materials. Eur. J. Pharm. Biopharm. 43, 138–141.

Cole, E.T., Rees, J.E., Hersey, J.A., 1975. Relations between compaction data for some crystalline pharmaceutical materials. Pharm. Acta Helv. 50, 28–32.

Duberg, M., Nyström, C., 1982. Studies on direct compression of tablets VI. Evaluation of methods for the estimation of particle fragmentation during compaction. Acta Pharm. Suec. 19, 421–436.

Farshad, M., Flüeler, P., 1998. Investigation of mode III fracture toughness using an anti-clastic plate bending method. Eng. Fract. Mech. 60, 597–603.

Farshad, M., Wildenberg, M.W., Flüeler, P., 1997. Determination of shear modulus and Poisson's ratio of polymers and foams by anticlastic plate bending method. Mater. Struct. 30, 377–382.

Fell, J.T., Newton, J.M., 1968. The tensile strength of lactose tablets. J. Pharm. Pharmacol. 20, 657–658.

Fell, J.T., Newton, J.M., 1970. Determination of tablet strength by the diametral-compression test. J. Pharm. Sci. 59, 688–691.

Griffith, A.A., 1920. The phenomena of rupture and flow in solids. Trans. Roy. Soc. Ser. A221, 163–198.

Humbert-Droz, P., Gurny, R., Mordier, D., Doelker, E., 1983. Densification behaviour of drugs presenting availability problems. Int. J. Pharm. Technol. Prod. Manufact. 4, 29–35.

Ichikawa, J.-I., Imagawa, K., Kaneniwa, N., 1988. The effect of crystal hardness on compaction propensity. Chem. Pharm. Bull. 36, 2699–2702.

Jetzer, W., Düggelin, M., Guggenheim, R., Leuenberger, H., 1984. Raster-elektronenmikroskopische Untersuchungen von Wechselwirkungen beim Verpressen von binären Pulvermischungen. Acta Pharm. Technol. 30, 126–131.

Johnson, K.L., 1997. Adhesion and friction between a smooth elastic spherical asperity and a plane surface. Proc. Roy. Soc. Lond. A. 453, 163–179.

Mashadi, A.B., Newton, J.M., 1987a. The characterisation of the mechanical properties of microcrystalline cellulose: a fracture mechanics approach. J. Pharm. Pharmacol. 39, 961–965.

Mashadi, A.B., Newton, J.M., 1987b. Assessment of the mechanical properties of compacted sorbitol instant. J. Pharm. Pharmacol. 39, 676P.

Mashadi, A.B., Newton, J.M., 1988. Determination of the critical stress intensity factor (K_{IC}) of compacted pharmaceutical powders by the double torsion method. J. Pharm. Pharmacol. 40, 597–600.

Menčík, J., 1992. Strength and Fracture of Glass and Ceramics. Elsevier, Amsterdam, p. 117.

Mielck, J.B., Stark, G., 1995. Tabletting of powder mixtures: parameters of evolved pressure-time profiles indicate percolation thresholds during tabletting. Eur. J. Pharm. Biopharm. 41, 206–214.

Pedersen, S., Kristensen, H.G., 1994. Change in crystal density of acetylsalicylic acid during compaction. STP Pharma. Sci. 4, 201–206.

Podczeck, F., 2001. Investigations into the fracture mechanics of acetylsalicylic acid and lactose monohydrate. J. Mater. Sci. 36 (19).

Rice, R.W., 1994. Porosity effects on machining direction—strength anisotropy and failure mechanisms. J. Am. Ceram. Soc. 77, 2232–2236.

Ridgway, K., Shotton, E., Glasby, J., 1969. The hardness and elastic modulus of some crystalline pharmaceutical materials. J. Pharm. Pharmacol. 21, 19S–23S.

Roark, R.J., 1965. Formulas for Stress and Strain, 4th ed. McGraw-Hill, New York, p. 194.

Rowe, R.C., Roberts, R.J., 1995. Mechanical properties. In: Aldeborn, G., Nyström, C. (Eds.), Pharmaceutical Powder Compaction Technology. Marcel Dekker, New York, pp. 283–322.

Stanley, P., 1985. Mechanical strength testing of compacted powders. In: Postgraduate School, Production Process on Tablet Manufacture. The Pharmaceutical Society of Great Britain, London, pp. 123–150.